

Article

Airborne Lidar: Advances in Discrete Return Technology for 3D Vegetation Mapping

Valerie Ussyshkin * and Livia Theriault

Optech Incorporated, 300 Interchange Way, Vaughan, ON L4K 5Z8, Canada; E-Mail: liviat@optech.ca

* Author to whom correspondence should be addressed; E-Mail: valerieu@optech.ca;
Tel.: +1-905-660-0808; Fax: +1-905-660-0829.

Received: 30 December 2010; in revised form: 9 February 2011 / Accepted: 10 February 2011 /
Published: 25 February 2011

Abstract: Conventional discrete return airborne lidar systems, used in the commercial sector for efficient generation of high quality spatial data, have been considered for the past decade to be an ideal choice for various mapping applications. Unlike two-dimensional aerial imagery, the elevation component of airborne lidar data provides the ability to represent vertical structure details with very high precision, which is an advantage for many lidar applications focusing on the analysis of elevated features such as 3D vegetation mapping. However, the use of conventional airborne discrete return lidar systems for some of these applications has often been limited, mostly due to relatively coarse vertical resolution and insufficient number of multiple measurements in vertical domain. For this reason, full waveform airborne sensors providing more detailed representation of target vertical structure have often been considered as a preferable choice in some areas of 3D vegetation mapping application, such as forestry research. This paper presents an overview of the specific features of airborne lidar technology concerning 3D mapping applications, particularly vegetation mapping. Certain key performance characteristics of lidar sensors important for the quality of vegetation mapping are discussed and illustrated by the advanced capabilities of the ALTM-Orion, a new discrete return sensor manufactured by Optech Incorporated. It is demonstrated that advanced discrete return sensors with enhanced 3D mapping capabilities can produce data of enhanced quality, which can represent complex structures of vegetation targets at the level of details equivalent in some aspects to the content of full waveform data. It is also shown that recent advances in conventional airborne lidar technology bear the potential to create a new application niche, where high quality dense point clouds, enhanced by fully recorded intensity for multiple

returns, may provide sufficient information for modeling and analysis, which have traditionally been applied mostly to full waveform data.

Keywords: lidar; airborne; discrete returns; full waveform; 3D vegetation mapping

1. Introduction

For over two decades airborne lidar technology has been successfully used for various 3D mapping applications including vegetation and forestry research. One of the first attempts to use airborne lidar for vegetation mapping was reported by the Canadian Forestry Service, which demonstrated the applicability of profiling airborne lidar for the estimation of height and density of the forest canopy and the ground elevation underneath [1]. This and numerous subsequent studies showed that lidar measurements of vegetation canopy can be used to characterize vegetation vertical structure and derive various physical attributes used for academic research, environmental studies and natural resources management programs [2-6].

Early tests in the lidar mapping of complex vegetation and forest targets were done using non-commercial, custom-made lidar systems. Meanwhile, the mainstream of commercial lidar sector had been focused on “two-dimensional” topographic mapping, which means that only a single measurement in range domain is required to create lidar-derived surface elevation maps. It is for this reason the lidar sensors developed for commercialized topographic mapping applications are often referred as “conventional” in contrast with the early custom-built full waveform sensors with primary application focus on 3D vegetation mapping for research purposes. Early commercial lidar systems had the ability to capture only two discrete returns for each emitted laser pulse [7]. This feature, though seemingly modest compared with today’s advanced lidar systems, provided enriched information for new applications with some elements of 3D data analysis such as feature extraction in forested [8] or urban areas [9]. With further development of conventional lidar technology, more advanced sensors capable of capturing up to four range and four or three intensity returns became commercially available (such as ALTM series of Optech Incorporated, ALS series of Leica Geosystems) that created more application niches of 3D data analysis including flood modeling, classification of bare-earth ground *versus* elevated features, vegetation-removal, certain feature extraction, power line modeling [10-13]. In particular, sensors with multiple-return capabilities have proven to be very efficient among different remote sensing techniques to characterize the ground topography as well as forest structure [14,15]. Numerous studies on vegetation mapping applications based on the use of conventional lidar systems have been reported [15,16].

However, due to the limited number of measurements in vertical domain provided by conventional sensors, and complexity of the vertical structure of vegetation targets, full waveform technology with unlimited number of measurements per every emitted laser pulse has often been perceived as a preferable choice for some 3D vegetation mapping applications [14,16]. The following section gives an overview on advantages and limitations of using both types of sensors for 3D vegetation mapping focusing on specific sensor characteristics important for this application.

2. Background

2.1. Discrete Return and Full Waveform Systems

Lidar sensors currently used for 3D vegetation mapping and forestry research can be categorized as either discrete return (DR) or full waveform (FW) systems [16,17]. They differ from one another mainly with respect to the range measurement method, which implies significant differences in sensor hardware design. On the application side, it results in distinctively different number of range measurements recorded for each emitted laser pulse and subsequent substantial differences in data processing and analysis tools. As a result, the data collected by DR and FW sensors representing the same 3D vegetation target may look dramatically different [17].

Most commercially available DR sensors allow for a few, typically four, multiple returns to be recorded for each emitted laser pulse. A FW lidar measures the full profile of a return signal by sampling it in fixed time intervals, typically 1 ns (equivalent to 15 cm sampling distance), with theoretically unlimited number of measurements per every emitted pulse. Practically, the number of recorded measurements is determined by several factors including sensor hardware and data flow design and may be limited by a number from a few tens to a few hundreds of measurements. This provides a quasi-continuous recording of the reflected energy for each emitted laser pulse. It is often perceived to create a “true” profile representing the vegetation canopy structure [16] as opposed to DR sensor measurements providing only up to four records typically separated by a few meter distances (Section 2.2). However, due to the limited capabilities of processing and analysis software for FW data, more data does not always translate into more or better information for data interpretation [17].

The information content of the returned laser signal also depends on characteristics of the horizontal illuminated area (laser footprint) [16]. The most common commercial sensors are small-footprint systems, either DR or FW sensors. Some manufacturers offer sensors capable of both operational modes: the main DR sensor and an optional FW unit, which may or may not be used during data collection missions [17].

Each data collection mode, either FW or DR, has distinct advantages and disadvantages that vary depending upon the applications [16]. Most commercial DR systems can provide extremely high ground point density. This enables the high-resolution representation of complex targets in the horizontal plane with a somewhat coarsely resolved elevation structure. These characteristics make DR sensors a perfect choice for “two-dimensional” topographic mapping. However, the coarse resolution of measurements in vertical domain—typically a few meters—has often limited the use of conventional lidar sensors for some 3D mapping applications, particularly for analysis of vegetation canopies [16]. On the other hand, FW technology has often been considered as the preferable choice for most comprehensive characterization of vegetation canopy [16,18]. It has been demonstrated that FW data provide a more complete and accurate assessment of the vegetation canopy and potential obstruction detection than DR data [19]. Moreover, FW data capture gives the user much more flexibility and control in the data processing and interpretation steps [20]. However, dealing with FW datasets takes lidar data handling to a drastically higher level of complexity compared with conventional DR point cloud data. First, the volume of FW data is overwhelming [20,21]. Moreover, there are neither commercial nor open-source toolkits to handle FW lidar data, but only custom-made solutions typically

designed for specific sensors [22]. Therefore, handling, interpretation and analysis of full-waveform lidar data is a complicated and expensive task. This often limits the commercial use of FW data. It also delayed the full commercialization of FW technology, which only recently began emerging to the commercial sector [23,24].

However, the rich content of FW data acquired at a high sampling rate, which is important for analysis of complex 3D targets, has limited value for broad area topographic mapping where only a few discrete returns are needed to create a digital elevation map. That is why the main application focus of FW technology remains in forestry and vegetation research and it remains unclear if it might be useful outside these applications [25].

2.2. Vertical Target Discrimination Distance

As mentioned above, the number of multiple returns in a DR sensor, as well as the sampling rate of a FW sensor, is not the only factor to determine the information content of lidar data comprising complex 3D targets. Since the recorded signal represents a convolution of the sensor waveform and the backscattering cross-section of the illuminated target [26], the emitted laser pulse characteristics and sensor receiver design have a big impact on the lidar data comprising complex targets irrespective of the sensor operational mode, either FW or DR. There are numerous studies on FW data analysis based on filtering and decomposition of recorded profiles with the purpose of eliminating data interpretation errors due to influence of the sensor waveform [26-28]. However, the effect of DR sensor waveform on the data comprising complex vertical targets is often overlooked, which may result in misinterpretation of DR data. Particularly, the DR sensor waveform determines the range measurement resolution, which is one of the most important characteristics determining the information content of DR data comprising complex vertical targets.

In most commercial DR lidar systems, the range measurement resolution is about 2.0–3.5 m, which produces gaps in the measurements along the sensor line of sight. These gaps are often referred to as “dead zones”, which means that the sensor receiver is not capable of detecting the next consecutive range return within certain time interval after the previous measurement is taken. The equivalent length of the “dead zone” in time domain is one of the internal characteristics of DR sensor and determined solely by the hardware design, mainly through characteristics of the emitted laser pulse and receiver electronics, *i.e.*, sensor waveform. On the practical side this parameter translates to the minimum vertical target discrimination distance. It means that 3D structure details separated by any distance less than this minimum cannot be resolved by consecutive range measurements along the sensor line of sight irrespective of physical properties of illuminated targets. That’s why it could be characterized empirically as minimal distance between consecutive DR returns for each emitted laser pulse (minimal pulse separation distance).

Until recently, minimal vertical target discrimination distances were not specified in the data sheets of most commercial lidar systems. This situation created some misunderstanding in the lidar community while some users expected to get multiple returns from vegetation without considering this parameter. Not accounting for the coarse resolution of range measurements may also lead to gross systematic errors caused by faulty interpolation.

With FW sensors, the high measurement sampling rate is often misinterpreted as the sensor capability to resolve vertical details with high resolution. However, for FW sensors, as well as for DR, vertical target resolution capability could be estimated through the emitted laser pulse width [24] and it is practically unrelated to the range measurement sampling rate. Very complicated decomposition algorithms applied to FW data may help to go beyond the vertical resolution limit of the lidar sensor [27]. It has been reported [28] that specially developed filtering algorithms applied to FW data recorded in a specially designed experiment with the use of emitted laser pulses of different characteristics resulted in distinguishing target features with a step smaller than ten times of the pulse length. In some particular cases special analysis techniques applied to repetitive observations of the same target over different time periods may help to detect small changes in vertical structure on a much smaller scale than even the sampling rate [29]. However, since the methods of FW data analysis which help to go beyond the sensor vertical resolution limit have not been commercialized, the mainstream of commercial lidar sector relies mostly on DR data and commercially available data analysis tools. That is why the capability of DR sensors to resolve vertical structure details is one of the key factors important for 3D vegetation mapping in the commercial lidar sector.

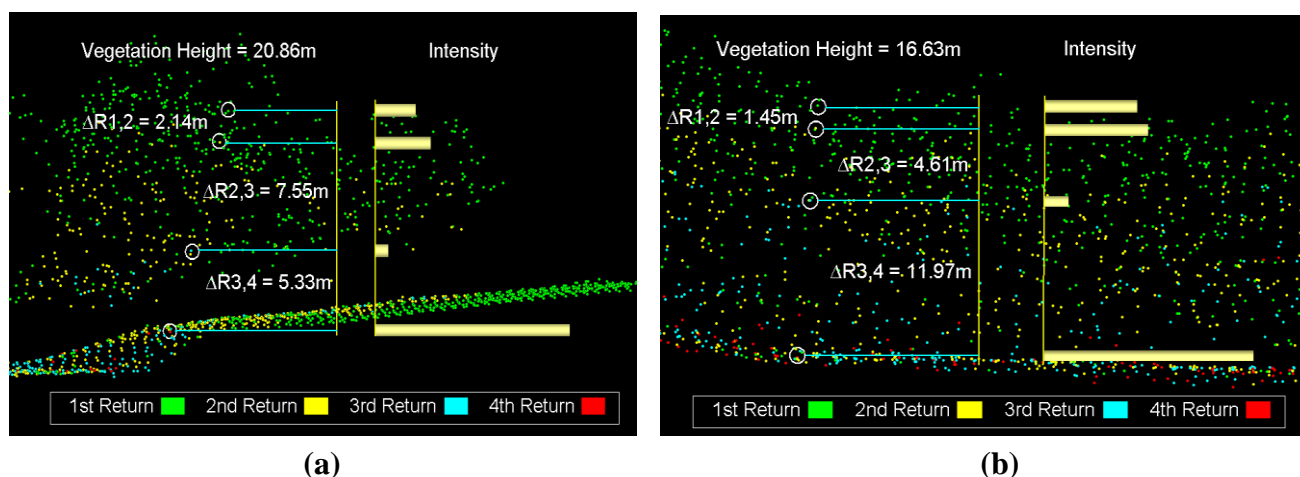
The following sections present an overview on the evolution of certain features of DR airborne lidar technology relevant to 3D mapping applications using the ALTM series of airborne sensors manufactured by Optech Incorporated as an example. The recent study on advanced capabilities of the ALTM-Orion, a new-generation DR airborne sensor, is presented and discussed in the context of 3D vegetation mapping applications.

3. Enhancing Capabilities of DR Technology for 3D Vegetation Mapping

Early commercial airborne lidar systems, such as Optech's ALTM 1020, 1210 and 1225 models manufactured between 1993 and 1998, had the ability to capture only two returns for each emitted laser pulse. These models were used mainly for topographic mapping applications with limited use for 3D analysis. With further evolution of this technology, more advanced ALTM models capable of capturing four range and four intensity returns became commercially available (such as ALTM 3100 and Gemini introduced to the commercial lidar sector between 2004 and 2006). Although most ALTM models can be integrated with a FW unit, the following discussion is focused only on the DR sensors and its features relevant to 3D vegetation mapping.

Figure 1(a,b) shows typical examples of multiple return vegetation data of two ALTM systems, 3100 and Gemini, which represent the most advanced models of the previous-generation ALTM series. Although in both selected examples the minimal pulse return separation distances are relatively small, 1.5–2.2 m, it is apparent that only four discrete returns with a few-meter separation between them cannot represent the vertical structure of vegetation properly. It was one of the reasons that until recently FW sensors have often been the preferable choice for some vegetation mapping applications, such as forestry research. However, the recent advances in DR lidar technology represented by a new generation ALTM model, ALTM-Orion, may change some aspects of this situation.

Figure 1. Examples of four-return records from vegetation; (a) ALTM 3100; minimum pulse return separation distance of 2.14 m; (b) ALTM Gemini: minimum pulse separation distance of 1.54 m.



The ALTM-Orion represents a radical departure from previous generations of airborne lidar sensors. First, the physical form factor—size and weight—has been reduced by a whole order, making the ALTM-Orion the first ultra-compact complete lidar solution with an optional UAV (unmanned aerial vehicle) configuration [30]. Second, it has been shown [31] that the performance characteristics of the ALTM-Orion include a few centimeter data elevation accuracy and precision for solid targets, as well as for the data comprising small-size linear targets such as wires in power line corridors. In addition, the new advanced design of the sensor transmitter and receiver hardware enabled to reduce the minimal vertical target discrimination distance to sub-meter level, which has never been available before in any commercial DR airborne lidar. In order to evaluate the performance and characterize the enhanced capabilities of ALTM-Orion important for 3D vegetation mapping application, Optech Incorporated has launched a series of studies presented below.

3.1. Objectives and Methodology

For the purpose of this study we selected several datasets collected by ALTM-Orion at 500 m flying altitude over different types of vegetation targets. The ground point density was about 12 ppm^2 ; the laser pulse repetition frequency (equal to data collection rate) was kept at the maximum of 200 kHz for all datasets. This study is based on the data collected over three areas of vegetation: a cornfield with an average height 2.2–2.8 m and two nearby mixed forested areas with an average height of 6–7 m on one side of the cornfield and 20–22 m on the other side. For the purpose of this study these datasets will be referred in this paper as low-, medium- and high-canopy vegetation data. All datasets were collected by the same ALTM-Orion system during the same data collection mission.

The objectives of this study include:

1. Empirical evaluation of the minimum vertical target discrimination distance for ALTM-Orion data using statistical analysis of the field data collected over selected types of vegetation targets.

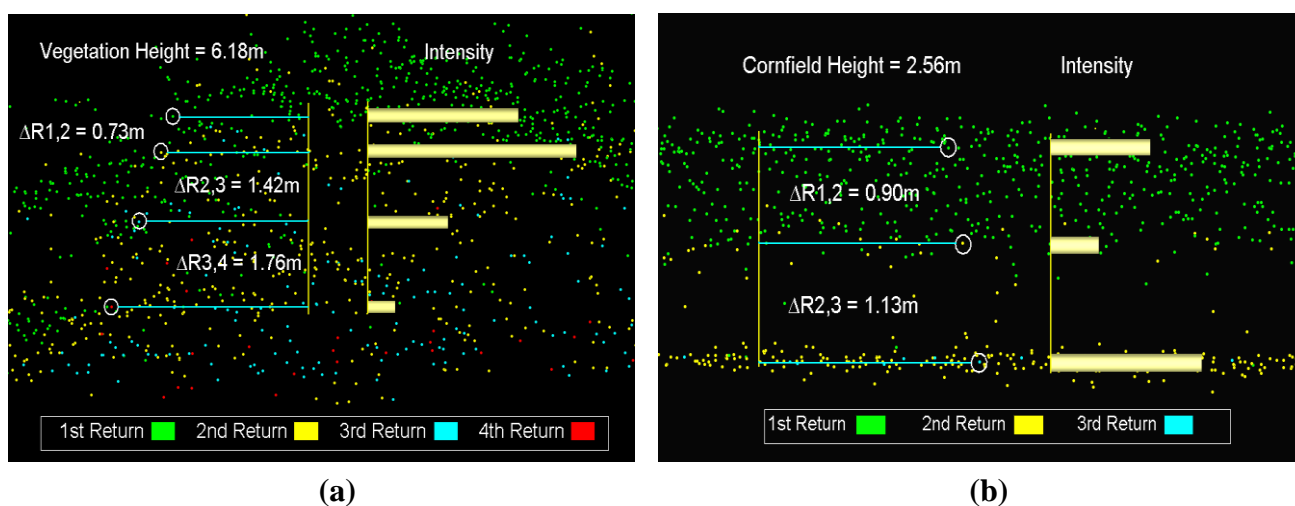
2. Analysis of the capabilities of ALTM-Orion to represent the vertical structure of vegetation targets: number and distribution of multiple returns, typical vertical target discrimination values, correlation of number of multiple returns with vegetation height, signal penetration to the ground.
3. Comparison of the results of 1–2 to a similar analysis based on ALTM-Gemini data.
4. Investigate the potential of return signal waveform modeling for DR data.

In order to achieve the aims of 1–3, several datasets of processed ALTM data were analyzed using basic statistical tools, while lidar software visualization tools, such as Terrascan, were used for verification and illustration of the results. The approach used for the return waveform modeling based on analysis of DR data as well as some preliminary results and discussion, are presented in Section 4 describing the second part of this study.

3.2. Results and Discussion

Figure 2(a) shows an example of ALTM Orion data collected over 6 m high vegetation illustrating four multiple returns for one emitted laser shot with the minimum pulse return separation distance of 73 cm. Figure 2(b) shows a similar sample record of three consecutive returns with sub-meter separation distances in the cornfield data with average height in that location of 2.6 m. It is quite remarkable that in spite of such a small height and high density of the crop, the ALTM Orion was still capable to detect three consecutive returns with the last one showing strong intensity representing the ground return.

Figure 2. ALTM-Orion data: (a) A four-return record for one emitted laser pulse over 6 m high mixed forest; (b) A three-return record for one emitted laser pulse over 2.6 m high cornfield.



In order to determine the minimal vertical target discrimination distance achievable by ALTM-Orion, the multiple return data collected over the entire cornfield were statistically analyzed in three randomly selected samples. Table 1 presents a statistical summary of average and minimum pulse separation distances in multiple returns for these samples.

Table 1. ALTM-Orion: Average and minimal multiple return separation distances for the cornfield data; the last column shows the average vegetation height in the selected samples.

Sample	Avg $\Delta R_{1,2}$ (m)	Avg $\Delta R_{2,3}$ (m)	Avg $\Delta R_{3,4}$ (m)	Avg height (m)
1	1.36	1.06	n/a	2.31
2	1.25	0.99	n/a	1.92
3	1.34	1.00	n/a	2.12
Sample	Min $\Delta R_{1,2}$ (m)	Min $\Delta R_{2,3}$ (m)	Min $\Delta R_{3,4}$ (m)	Avg height (m)
1	0.67	0.69	n/a	2.31
2	0.64	0.65	n/a	1.92
3	0.66	0.67	n/a	2.12

This summary clearly indicates that the minimal pulse return separation distances of ALTM-Orion consistently fall within 0.64–0.67 m interval for all multiple returns. It also shows that there was no single incidence of four-return record in all three samples of the cornfield data. This observation, which may seem to be obvious, is in fact a clear indication that the number of multiple returns in vegetation data is determined by the ratio between the vegetation height and minimum vertical target discrimination capability of the lidar sensor.

Comparing the variations in average pulse return separation distances with changes in the total cornfield height from sample to sample, one can also conclude that the second return R2 may be an indicator of a change in the cornfield vertical structure while the last return R3 clearly indicates the ground return. This is confirmed by the example of a three-return record presented in Figure 2(b), which also shows that the second return, if detected from the middle of the cornfield mass, would have the lowest intensity. All of this makes it possible to map the vertical structure of the cornfield based solely on the information derived directly from discrete return data. Figure 3 shows color-coded representation of the cornfield vertical structure derived directly from the processed DR data showing variations in density and height of the cornfield stalks, which could be used to for further characterization of the surveyed cornfield. This example shows that the enhanced capability of the ALTM-Orion to generate spatial data so rich in content enables the users to take DR data analysis to a different level with quantitative characterization of various attributes of this type of vegetation (height, structure, *etc.*).

Figure 3. Color-coded representation of the confined vertical structure based on processed DR data.

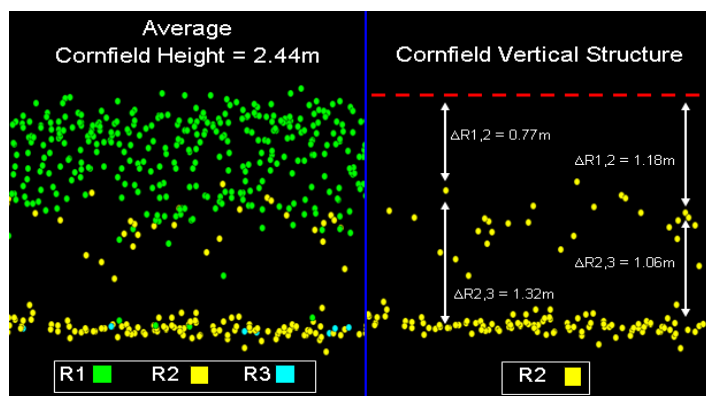


Table 2 shows a similar statistical summary for minimal and average pulse return separation distances for the other datasets collected over mixed vegetation with average height of 6–7 m and 20–22 m. Comparing these results with those ones presented in Table 1, it is evident that the minimum pulse return separation distances are not affected by the vegetation height and type and still fall mostly within the same range 0.6–0.7 m. This indicates that this parameter does represent the system capabilities rather than vegetation characteristics. On the other hand, average pulse separation distances, and more significantly, number of multiple returns, are affected by the vegetation height and type. This fact demonstrates that the resolution of the range measurements of a lidar system determines the number of multiple returns over a vertical target, if a few discrete returns are covering the full vertical extent of that target.

Table 2. ALTM-Orion: Average and minimum multiple return separation distances for the forest data; the last column shows the average vegetation height in the selected samples.

Sample	Avg $\Delta R_{1,2}$ (m)	Avg $\Delta R_{2,3}$ (m)	Avg $\Delta R_{3,4}$ (m)	Avg height (m)
1	2.54	2.10	1.91	6.0
2	3.64	3.92	4.26	22.5
3	3.44	3.50	3.69	20.0
Sample	Min $\Delta R_{1,2}$ (m)	Min $\Delta R_{2,3}$ (m)	Min $\Delta R_{3,4}$ (m)	Avg height (m)
1	0.68	0.71	0.73	6.0
2	0.70	0.70	0.64	22.5
3	0.65	0.61	0.68	20.0

In order to correlate the vegetation height and the number of multiple returns, we ran another type of statistical analysis for the mixed forest data. Table 3 presents the percentage of each multiple return in the same randomly selected samples of the vegetation data.

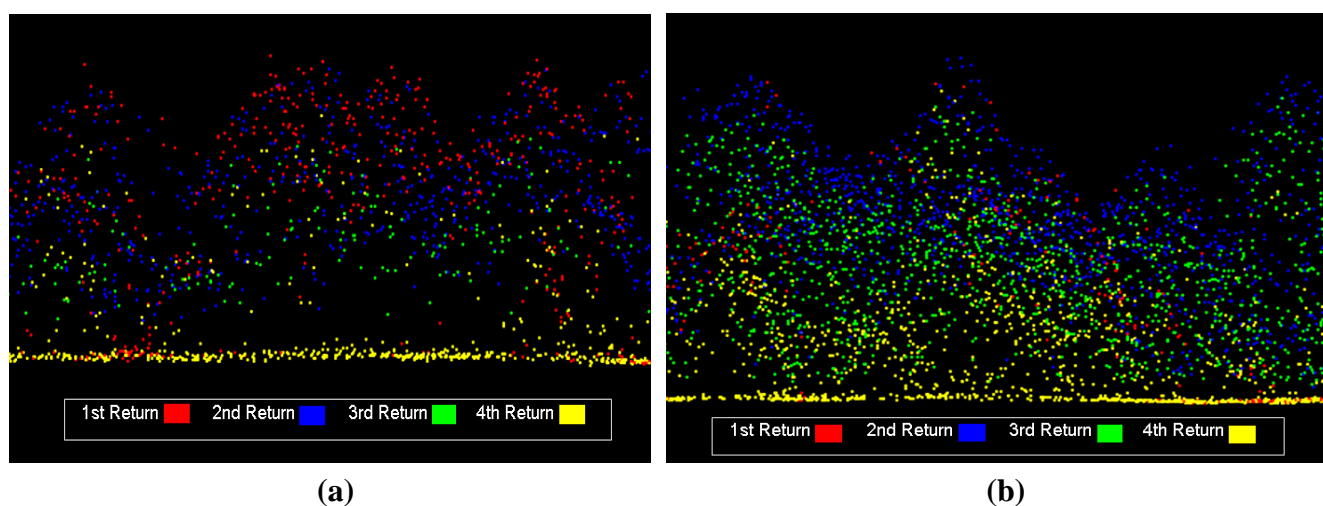
Table 3. ALTM-Orion: Distribution of multiple returns for the mixed forest data.

Sample	Pulse Return	% of Total
Sample 1 Average height 6 m	1	55.88
	2	33.03
	3	9.38
	4	1.71
Sample 2 Average height 22.5 m	1	43.22
	2	31.6
	3	17.71
	4	7.47
Sample 3 Average height 20 m	1	44.8
	2	31.91
	3	16.79
	4	6.51

First of all, this analysis confirms the correlation of the number of multiple returns with the vegetation height, which was evident from the data presented in Tables 1 and 2: there are no fourth returns in the cornfield data, while the system can consistently detect four returns from the vegetation of 6 m height or more while operating at the same altitude with the same data collection parameters during the same mission. Second, the numbers in Table 3 show that even small variations in the vegetation height affect the number of the last returns and the distribution of multiple returns within each data sample: the taller the vegetation canopy, the more third and fourth returns are detected. Moreover, small variations the vegetation height (Samples 2 and 3, Table 3) are significant enough to affect the distribution of the last returns.

In order to emphasize the significance of the advanced capabilities of the new-generation DR lidar for 3D vegetation mapping, the data collected by this system were compared to the vegetation data collected by the previous model of ALTM, Gemini. Some of the results of this comparison are presented below. Figure 4(a,b) shows a descriptive illustration of the difference, which makes sub-meter vertical target resolution for 3D vegetation data collected by a DR lidar. It represents the images of vegetation data collected by ALTM-Gemini and Orion systems over the same area around the same time of the year; the average canopy height is 15–17 m in both datasets. Both systems operated at the same laser pulse repetition frequency (equal to data collection rate) of 100 kHz, and at an altitude close to 1 km, which produced similar ground point density of 1.5–2.0 ppm² for both datasets.

Figure 4. Vegetation canopy of 15–17 m average height represented by multiple return data collected by two ALTM models operating at the same operational settings. (a) ALTM-Gemini; (b) ALTM-Orion.



This example clearly shows the advantage of the ALTM Orion's much smaller vertical target discrimination distance, which produces a better representation of the vegetation canopy structure as substantially more multiple returns are detected from the lower layers of vegetation. It is also important to note that there is virtually no gap between the ground and the low canopy returns in ALTM-Orion data that are often seen in similar images produced from data collected by other lidar sensors.

Table 4 represents a statistical summary similar to Table 3 for the data collected by ALTM-Gemini over the same type of vegetation of different height from 1-km flying altitude, and producing ground point density 1.5–2.0 ppm². The range measurement resolution of this sensor, determined by the

system hardware design, depends on the sequential number of the multiple returns and varies within 1.5–2.5 m [32]. Based on the distribution of the multiple returns in this case, one can conclude that for a tall vegetation canopy of 22–27 m, all four discrete returns are recorded, including the last one from the ground beneath the vegetation canopy; the percentage of third and fourth returns is substantial. However, for low-canopy vegetation of 6–7 m, the system cannot detect all four returns because of the 2.5 m minimal vertical target discrimination limit. The percentages of third and fourth returns for these samples are negligible as the system cannot resolve any two targets in vertical domain within a distance less than 2.5 m for the last two returns.

Table 5. ALTM-Gemini: Distribution of multiple returns for high and low-canopy vegetation.

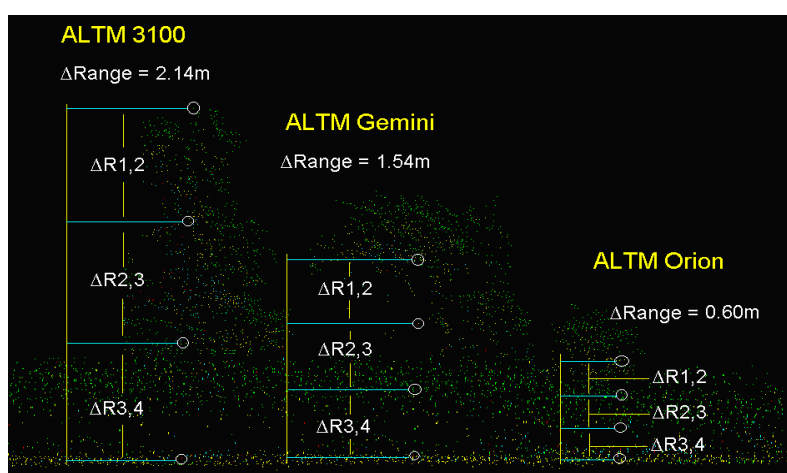
Pulse Return	Sample	% of Total	Sample	% of Total
1		84.5		43.5
2	Sample 1	15.3	Sample 4	35.3
3	Average height 6–7 m	0.2	Average height 22–27 m	16.9
4		0.0		4.3
1		85.7		39.8
2	Sample 2	14.1	Sample 5	31.9
3	Average height 6–7 m	0.2	Average height 22–27 m	21.4
4		0.0		6.9
1		83.6		42.1
2	Sample 3	15.8	Sample 6	34.0
3	Average height 6–7 m	0.6	Average height 22–27 m	18.7
4		0.0		5.2

The analysis presented above for two different ALTM models and for various types and height of vegetation indicates that for DR lidar systems the number of returns from the vegetation canopy are often limited not only by the density of vegetation, but also by the vertical target discrimination distance. That is why some of the observations of low percentages in third and fourth returns from vegetation [16] might have been the result of the system’s limited ability to resolve vertical vegetation structure, rather than the characteristic of an “optimal number” of echoes per pulse in a DR lidar being limited to three or another number. The examples shown indicate that the same DR sensor with coarser vertical target discrimination capabilities can detect a substantial percentage of returns as third and fourth echoes for tall vegetation, but cannot do the same for low- or medium-height vegetation because of limited resolution in consecutive discrete return measurements in the vertical domain. On the other hand, the new-generation DR sensor can consistently detect three returns from 2.5 m high crop and four returns over 6 m high vegetation with substantial numbers of multiple returns from the lower layers of the canopies as well as ground returns.

Figure 5 summarizes the evolution of vertical target discrimination capabilities in ALTM series of airborne sensors. It shows a clear trend towards a sub-meter scale of vertical target discrimination distance, which is achieving 60 cm values in the new-generation DR sensors. It could be considered as

a new level of capability of airborne DR technology to “sample” vertical structure of vegetation targets on the scale approaching the typical sampling interval, 15 cm, provided by FW technology. Although the technology of this “sampling” is different for DR and FW sensors, the dramatic improvement in vertical target discrimination capabilities of new-generation DR sensors may indicate a trend towards potential fusion of both types of lidar technology on the application side of 3D mapping. Moreover, it will be shown in the next section that by combining the information from range and intensity data collected by an advanced DR sensor, a simplified waveform analysis can potentially be applied to DR data in a way that is similar to that of FW data. Then the similarity in data analysis tools may also become another factor bridging some application niches of both types of lidar technology.

Figure 5. Evolution of minimal vertical target discrimination capabilities for ALTM series of airborne lidar sensors.



Summarizing this part of the study, it is important to note that the analysis presented above has been designed for the ultimate purpose of evaluation and demonstration of the advanced capabilities of the new generation DR airborne sensors relevant to 3D vegetation mapping. Although it provides insight on the potential use of DR data of enhanced quality for forestry, agricultural and environmental applications, scientific research on the properties and attributes of vegetation targets are out of scope of this paper.

The next section represents the second part of the study, which investigates the potential of applying simplified waveform modeling to discrete return data in a similar way to that of full waveform data.

4. Waveform Modeling for DR Data

The simplified waveform modeling of discrete multiple returns presented below is based on the approach similar to those used for full waveform data analysis, where extracted relevant signal peaks were modeled as analytical functions, typically, Gaussian [14,24]. Since the discrete return data used in our analysis represent the peaks of partial signal returns, we assumed that the entire reflected laser pulse energy could be decomposed into a sum of the components, while each one would be represented by a single discrete return:

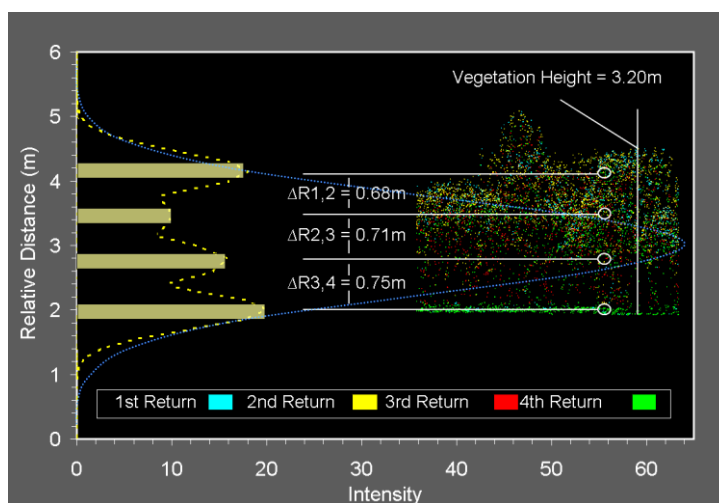
$$f(x) = \sum_{i=1}^n f_i(x) \tag{1}$$

Here $n = 4$ for four returns or 3 for three returns. For modeling of each function f_i in our analysis we used only a simple three-parametric Gaussian for all partial return for all vegetation types:

$$f_i = a_i \exp\left(-\frac{(x - \mu_i)^2}{2\delta_i^2}\right) \tag{2}$$

Figure 6 shows a graphic representation of our approach, where each discrete return is interpreted as a peak of a simple Gaussian (2) so that the amplitude of each Gaussian, a_i , was proportional to the recorded intensity values of each discrete return i , while the entire reflected laser pulse energy (blue Gaussian curve) represents the sum of all four DR components (1).

Figure 6. Graphic representation of the modeling approach of ALTM-Orion data.



The relative distances between the discrete returns were used for the μ_i parameter to determine the center position of each peak. The Gaussian pulse width, δ_i , was the fitting parameter, which was first estimated based on the system hardware parameters (laser pulse width, receiver bandwidth) and after that adjusted through the modeling described below. This step in the described methodology is based on the fact that the echoes reflected from different type of targets represent the convolution of the functions of the emitted laser pulse waveform, system receiver bandwidth and scattering properties of the targets [24,26]. In our simplified approach, we assumed that each one of the partial returns including ground and canopy returns could be approximated by simple three-parametric symmetrical Gaussian (2) function. Then the pulse widths, amplitudes and positions of the modeled Gaussians for each discrete return would fully determine the waveform of the modeled signal profile over the vertical extent of the target.

Furthermore, we assumed that the superposition (1) of all four (or three) simple Gaussian functions representing the waveforms of the discrete partial returns would represent the total optical receiver power P_r , which connected to the transmitted optical power P_t and can be modeled through the lidar

equation [33]. Considering partial signal returns P_i , the intensity (peak power) of each Gaussian pulse was modeled using the lidar equation in the form derived by Jelalian [34]:

$$P_i = \frac{P_r D_r^2 Q}{4\pi \mathcal{G}^2} T_{atm}^2 \frac{\sigma_i}{R_i^4} \quad (3)$$

Here:

P_i is the received signal power for i -return

P_r is the transmitted laser pulse power

D_r is the diameter of the lidar receiver aperture

Q is the optical efficiency of the lidar system

\mathcal{G} is the laser beam divergence

T_{atm} is the atmospheric transmittance factor

R_i is the range from the sensor to i -target

σ_i is the effective backscattering cross-section of i -target

Here the reflective properties of each target for each partial return P_i are described by the backscattering cross-section σ_i , which is proportional to the i -target reflectance ρ_i and the i -fraction of the total received power P_r in each return:

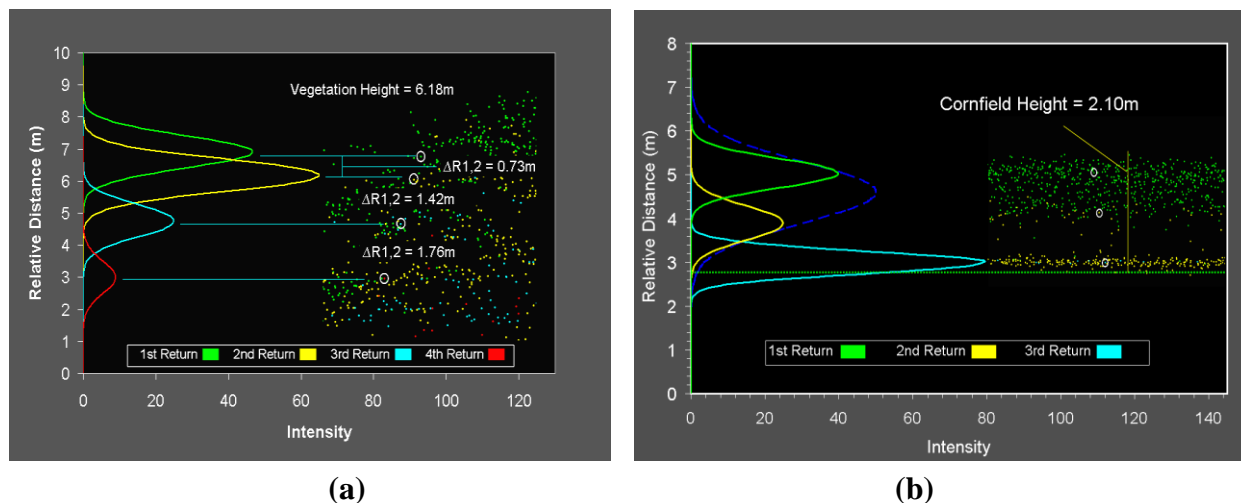
$$\sigma_i = k_i \rho_i A_i \quad (4)$$

Here A_i is the area of the target illuminated by the i -fraction of the laser footprint, which created the discrete return f_i and k_i is the fitting parameter, characterizing scattering properties of i -target, which could be derived using redundant measurements. An approach similar in some aspects to this one was applied to the analysis of full waveform data by Wagner and co-authors [24,35,36].

Based on the approach described by Equations (1–4), and using the known characteristics of the ALTM-Orion hardware (emitted laser pulse characteristics, parameters of the receiver electronics and optics), it was possible to model the total return optical power P_r through the lidar equation for a single laser shot. Since P_r was assumed to be a superposition of all four (or three) partial returns P_i with a simple Gaussian waveform, and knowing the intensities for each discrete return, it was possible to model the amplitudes a_i and pulse widths δ_i of each discrete return for the selected laser shots so that the sum of the return pulse energies of all partial returns P_i would represent the pulse energy of the total return P_r . Figure 7 illustrates the results of the Gaussian waveform modeling for the samples of multiple returns of the vegetation data presented earlier in Figure 2.

For such a consistent target as cornfield (Figure 7(b)) it also seemed to be possible to estimate the effective reflectivity of the cornfield stalks through the Gaussian modeling of the corn and ground returns. The blue dashed line in this figure represents the theoretical sum return that encompasses two returns from vegetation, corn stalks, as opposed to the ground return with different reflective properties. The histogram analysis of the intensity data consisting only of the same number of returns (one, two or three returns) and reflected from the same type of target (corn as opposed to the ground) showed consistent quasi-normal distribution of intensity values over sampled datasets. This work is still in progress and requires more detailed analysis, but the preliminary results partly presented here demonstrate a new potential of DR data analysis, which could potentially bridge the data analysis tools used for both types of lidar technology.

Figure 7. Illustration of the waveform modeling for ALTM-Orion data: (a) mixed vegetation data (refer to Figure 2(a)); (b) cornfield data (refer to Figure 2(b)).



The discrete return data analysis described above resembles, in many aspects, and relies on, the methodologies applied to full waveform data analysis and reported by leading experts in the field (Wagner, Jutzi, Chauve and Bretar and their co-authors quoted earlier in this paper) and might be used in applications similar to those which up to date have been considered as belonging solely to full waveform technology. Moreover, since the simple Gaussian function used in this type of analysis is fully determined by the three parameters derived on the basis of single range and single intensity measurements for each discrete return, it appears that in some cases oversampling of the return signal profile with 1 ns (15 cm) interval may not add more details to the recorded profile of the vertical target. This conclusion is valid mostly for those cases when a few discrete returns separated by minimal vertical target discrimination distance of the lidar sensor are covering the full vertical extend of a consistent 3D target. By comparing the examples of ALTM-Orion data (Figure 2) and the corresponding modeled waveforms (Figure 7) with the real FW data with 1 ns sampling rate collected over similar vegetation targets by a FW airborne sensor [36], one can conclude that DR data of enhanced quality can represent vertical structure of these types of vegetation at the level of details equivalent to or even better than that of full waveform data.

This can be considered a potential fusion of two types of airborne lidar technologies on the application side of 3D vegetation mapping. Not only the level of details representing the vertical structure of vegetation provided by advanced DR sensors can be equivalent to that one provided by FW sensors, but also similar approaches could be used for the analysis of both types of data. However, full waveform technology will continue to be essential and irreplaceable for those applications, where the reflected pulse echoes are expected to have significantly different characteristics, comparing to the emitted pulse due to the interactions between the laser beam and complex targets [26], especially if the interception geometry results in large angles of incidence [37,38]. In these cases, the high sampling rate of the FW data would provide a much more reliable input for modeling waveforms and it may also help to resolve vertical targets on the scale beyond sensor range measurement resolution by applying special data analysis and processing algorithms.

Full waveform technology will also remain a preferable choice for 3D vegetation mapping that requires the analysis of tall vegetation canopies (e.g., mature forest), as long as the number of multiple discrete returns provided by advanced DR lidar systems is limited by four. In these cases only four multiple discrete returns would leave wide gaps in the modeled vertical canopy profile. However, with further development of DR and data handling technologies, when more than four discrete returns are supported by both the lidar system hardware and the format of output data, it may become possible for the DR and FW approach to give similar results in terms of representing 3D vegetation structure details for some applications. Then it may become possible to develop new automated data analysis tools for 3D vegetation mapping bridging the academic research based on full waveform data analysis with the workflow practices for discrete return data established in the commercial sector of lidar industry.

4. Conclusions

For the last two decades, the use of airborne lidar technology in certain 3D vegetation mapping applications has often been based on analysis of the canopy profiles recorded by full waveform sensors. The use of discrete return sensors for detailed representation on vertical vegetation structure has been limited because of the coarse resolution of range measurements. The evolution of discrete return lidar technology has achieved a new level of capabilities that approach those of full waveform technology in representing 3D vegetation structure. The substantial reduction in vertical target discrimination distance of new generation discrete return sensors may indicate a trend towards potential bridging of both types of lidar technology on the application side of 3D vegetation mapping. The trade-off between the high complexity and costs associated with full waveform data handling and analysis on the one hand, and discrete return data of enhanced quality on the other hand, has the potential to create a new application niche in the lidar industry with possible fusion of data analysis tools for both types of lidar data. In this niche, high-quality dense discrete return point clouds, with fully recorded intensity information for each of the multiple returns, may provide sufficient information for automated modeling, analysis and quantitative characterization of 3D vegetation structure for a variety of applications.

Acknowledgements

The authors are grateful to Brent Smith and Eric Yang for fruitful discussions.

References

1. Aldred, A.; Bonner, M. *Application of Airborne Lasers to Forest Surveys*; Information Report PI-X-51; Petawawa National Forestry Centre, Canadian Forestry Service: Petawawa, ON, Canada, 1987; p. 62.
2. Nelson, R.; Krabill, W.; Maclean, G. Determining forest canopy characteristics using airborne laser data. *Remote Sens. Environ.* **1984**, *15*, 201-212.
3. Dubayah, R.O.; Drake, J.B. Lidar remote sensing for forestry. *J. Forestry* **2000**, *98*, 44-46.
4. Nelson, R.; Parker, G.; Hom, M. A portable airborne laser system for forest inventory. *Photogramm. Eng. Remote Sensing* **2003**, *69*, 267-273.

5. Roberts, S.D.; Dean, T.J.; Evans, D.L.; McCombs, J.W.; Harrington, R.L.; Glass, P.A. Estimating individual tree leaf area in loblolly pine plantations using LiDAR-derived measurements of height and crown dimensions. *Forest Ecol. Manage.* **2005**, *213*, 54-70.
6. Hudak, A.T.; Evans, J.S.; Smith, A.M.S. Review: LiDAR utility for natural resource managers. *Remote Sens.* **2009**, *1*, 934-951.
7. Ussyshkin, V.; Theriault, L. Advances in Airborne Lidar Technology for Forestry and Other 3D Mapping Applications. In *Proceedings of the Regional ISPRS Conference: Latin American Remote Sensing Week (LARS)*, Santiago, Chile, 4–7 October 2010.
8. Hopkinson, C.; Sitar, M.; Chasmer, L.; Treitz, P. Mapping snowpack depth beneath forest canopies using airborne lidar. *Photogramm. Eng. Remote Sensing* **2004**, *70*, 323-330.
9. Alharthy, A.; Bethel, J. Heuristic Filtering and 3D Feature Extraction from Lidar Data. In *Proceedings of ISPRS Commission III, Symposium 2002 "Photogrammetric Computer Vision"*, Graz, Austria, 9–13 September 2002.
10. Bates, P.D.; Pappenberger, F.; Romanowicz, R. Uncertainty and risk in flood inundation modeling. In *Flood Forecasting*; Beven, K., Hall, J., Eds.; Wiley & Co.: New York, NY, USA, 1999.
11. Raber, G.T.; Jensen, J.R.; Schill, S.R.; Schuckman, K. Creation of digital terrain models using an adaptive Lidar vegetation point removal process. *Photogramm. Eng. Remote Sensing* **2002**, *68*, 1307-1316.
12. Renslow, M.; Greenfield, P.; Guay, T. *Evaluation of Multi-Return LIDAR for Forestry Applications*; RSAC-2060/4810-LSP-0001-RPT1; US Department of Agriculture Forest Service-Engineering: Salt Lake City, UT, USA, 2000; Available online: http://www.ndep.gov/USDAFS_LIDAR.pdf (accessed on 19 November 2010).
13. Ussyshkin, V.; Sitar, M. Advantages of Airborne Lidar Technology for Power Line Asset Management. In *Proceedings of 5th Annual CIGRÉ Canada Conference: Innovation and Renewal-Building the New Power System*, Vancouver, BC, Canada, 17–19 October 2010; [CDROM].
14. Chauve, A.; Mallet, C.; Bretar, F.; Durrieu, S.; Pierrot-Deseilligny, M.; Puech, W. Processing Full-Waveform Lidar Data: Modelling Raw Signals. In *Proceedings of ISPRS Workshop on Laser Scanning 2007*, Espoo, Finland, 12 September 2007; Volume 36, Part 3/W52, pp. 102-107.
15. Korpela, I.; Ørka, H.O.; Maltamo, M.; Tokola, T.; Hyyppä J. Tree species classification using airborne LiDAR—Effects of stand and tree parameters, downsizing of training set, intensity normalization, and sensor type. *Silva Fennica* **2010**, *44*, 319-339.
16. Lim, K.; Treitz, P.; Wulder, M.; St-Onge, B.; Flood, M. LiDAR remote sensing of forest structure. *Progr. Phys. Geogr.* **2003**, *27*, 88-106.
17. Parrish, C.E.; Scarpace, F.L. Investigation of Full Waveform Lidar Data for Detection and Recognition of Vertical Objects. In *Proceedings of ASPRS 2007 Annual Conference*, Tampa, FL, USA, 7–11 May 2007.
18. Chauve, A.; Vega, C.; Bretar, F.; Durrieu, S.; Allouis, T.; Pierrot-Deseilligny, M.; Puech, W. Processing full-waveform lidar data in an alpine coniferous forest: assessing terrain and tree height quality. *Int. J. Remote Sens.* **2009**, *30*, 5211-5228.

19. Magruder, L.A.; Neuenschwander, A.L.; Marmillion, S.P.; Tweddale, S.A. Obstruction detection comparison of small-footprint full-waveform and discrete return lidar. *Proc. SPIE* **2010**, 7684, 768410, doi:10.1117/12.850274.
20. Chauve, A.; Bretar, F.; Pierrot-Deseilligny, M.; Puech, W. Full Analyze: A Research Tool for Handling, Processing and Analyzing Full-Waveform Lidar Data. In *Proceedings of the 2009 IEEE International Geoscience and Remote Sensing Symposium (IGARSS)*, Cape Town, South Africa, 12–17 July 2009.
21. Ussyshkin, V.; Theriault, L. ALTM-Orion: Bridging Conventional Lidar and Full Waveform Digitizer Technology. In *ISPRS TC VII Symposium "100 Years ISPRS"*, Vienna, Austria, 5–7 July 2010; Volume 38, Part 7B, pp. 606–611 [CDROM].
22. Bretar, F.; Chauve, A.; Mallet, C.; Jutzi, B. Managing Full Waveform Lidar Data: A Challenging Task for the Forthcoming Years. In *Proceeding of XXIst ISPRS Congress*, Beijing, China, 3–11 July 2008; Volume 37, Part B1, pp. 415–420.
23. Neuenschwander, A.L.; Magruder, L.A.; Tyler, M. Landcover classification of small-footprint, full-waveform lidar data. *J. Appl. Remote Sens.* **2009**, 3, 033544.
24. Wagner, W.; Hollaus, M.; Briese, C.; Ducic, V. 3D vegetation mapping using small-footprint full-waveform airborne laser scanners. *Int. J. Remote Sens.* **2008**, 29, 1433–1452.
25. Petrie, G. Current Developments in Airborne Laser Scanning Technologies. In *Proceedings of IX International Scientific & Technical Conference—From Imagery to Map: Digital Photogrammetric Technologies*, Attica, Greece, 5–8 October 2009.
26. Jutzi, B.; Stilla, U. Characteristics of the Measurement Unit of a Full-Waveform Laser System. In *Symposium of ISPRS Commission I: From Sensors to Imagery*, Paris, France, May 2006; Volume 36, Part 1/A, [CDROM].
27. Reitberger, J.; Krzystek, P.; Stilla, U. Analysis of Fullwaveform LiDAR Data for Tree Species Classification. In *Proceedings of ISPRS Symposium of Commission III "Photogrammetric Computer Vision and Image Analysis"*, Bonn, Germany, 20–22 September 2006; Volume 36, pp. 228–233.
28. Jutzi, B.; Stilla, U. Range determination with waveform recording laser systems using a Wiener Filter. *ISPRS J. Photogramm. Remote Sens.* **2006**, 61, 95–107.
29. Hofton, M.A.; Blair, J.B. Laser altimeter return pulse correlation: A method for detecting surface topographic change. *J. Geodyn.* **2002**, 34, 477–489.
30. Hussein, M.; Tripp, J.; Hill, B. An ultra compact laser terrain mapper for deployment onboard unmanned aerial vehicles. *Proc. SPIE* **2009**, 7307, 73070B.
31. Ussyshkin, V.; Theriault, L. Precise Mapping: ALTM Orion Establishes a New Standard in Airborne Lidar Performance. In *Proceedings of ASPRS Annual Conference*, San Diego, CA, USA, 26–30 April 2010.
32. Ussyshkin, V.; Theriault, L. *Empirical Evaluation of the Resolution of Range Measurements in ALTM-Gemini*; Internal Optech Document; Optech: Vaughan, ON, Canada, 2010.
33. Measures, R.M. *Laser Remote Sensing, Fundamentals and Applications*; Wiley Interscience: New York, NY, USA, 1984.
34. Jelalian, A.V. *Laser Radar Systems*; Artech House: Boston, MA, USA, 1992.

35. Wagner, W.; Ullrich, A.; Ducic, V.; Melzer, T.; Studnicka, N. Gaussian decomposition and calibration of a novel small-footprint full-waveform digitising airborne laser scanner. *ISPRS J. Photogramm. Remote Sens.* **2006**, *60*, 100-112.
36. Wagner, W.; Ullrich, A.; Melzer, T.; Briese, C.; Kraus, K. From Single-Pulse to Full-Waveform Airborne Laser Scanners: Potential and Practical Challenges. In *Proceedings of the International Society for Photogrammetry and Remote Sensing 20th Congress Commission 3*, Istanbul, Turkey, 12–23 July 2004; Volume 35, Part B/3, pp. 6-12.
37. Schaer, P.; Skaloud, J.; Landtwing, S.; Legat, K. Accuracy Estimation for Laser Point Cloud Including Scanning Geometry. In *Proceedings of The 5th International Symposium on Mobile Mapping Technology*, Padua, Italy, 29–31 May 2007.
38. Jutzi, B.; Gross, H. Normalization of Lidar Intensity Data Based on Range and Surface Incidence Angle. In *Proceedings of Laserscanning 09*, Paris, France, 1–2 September 2009; Volume 38, Part 3/W8, pp. 213-218.

© 2011 by the authors; licensee MDPI, Basel, Switzerland. This article is an open access article distributed under the terms and conditions of the Creative Commons Attribution license (<http://creativecommons.org/licenses/by/3.0/>).